Fines Migration in Porous Media

A model developed by Sharma and Yortsos (1987a) is applied to the processes of fines migration and fines injection in a porous medium. The first is a problem frequently encountered in oil reservoirs when release of fines is triggered by physicochemical interactions of the porous formation with the injected fluids. The second may be a problem in the filtration of relatively large particulates. Simple solutions are provided for both processes by considering size exclusion as the dominant particle retention mechanism. The solutions developed provide expressions for the particle concentration profiles, the open pore density and pore size distribution profiles, as well as the permeability reduction. These expressions are of importance in the evaluation of the extent and depth of formation damage and can be used as designing tools for remedial treatment, such as acidizing or fracturing.

M. M. Sharma
Department of Petroleum Engineering
University of Texas
Austin, TX 78712

Y. C. Yortsos
Departments of Chemical
and Petroleum Engineering
University of Southern California
Los Angeles, CA 90007

Introduction

The migration of fine particles in a sandstone is triggered by the contact of the formation with an incompatible brine solution. The resulting formation damage has been the subject of some study over the past few decades. Typical experiments that dramatically illustrate this phenomenon were conducted by Jones (1964) and Gray and Rex (1966) and Mungan (1968). A several-fold reduction in the permeability was observed when a Berea sandstone core saturated with a 3% NaCl brine solution was flushed with brine solution, followed by the injection of distilled water. Upon reversing the flow direction, the original permeability was instantaneously recovered for a brief period of time; it subsequently dropped to very small values. The early literature on the subject (see review article by Moore, 1960) suggested that clay swelling was the dominant permeability reduction mechanism. However, it is now commonly accepted that fines migration in the form of clays or other fine particles is the major mechanism for permeability decline, even in the presence of swelling clays.

Recent studies by Khilar (1981), Khilar and Fogler (1983, 1984) and Khilar et al. (1983) have considerably enhanced the understanding of fines migration processes by delineating the effects of anions, cations, and pH of the injected solution permeability reduction. In particular, Khilar's work conclusively demonstrated:

- The existence of a critical salt concentration (CSC) beyond which the permeability of a sandstone varies with salinity
- The existence of a critical rate of salinity decline (CRSD) below which a permeability decline is not observed

The experimental results indicated that in the range of superficial velocities from 3.2 to 570.0 cm/h, the CSC was independent of the flow rate. Gruesbeck and Collins (1982), working with unconsolidated bead packs and actual cores reported that the fluid interstitial velocity determines to a large extent the rates of particle release. A critical flow velocity u_c was defined, above which the permeability was a linearly decreasing function of the fluid velocity, while below u_c a permeability reduction was not observed. A partial explanation of this apparent contradiction is provided by the recent work by Gabriel and Inamdar (1983). These authors distinguish between chemically induced and mechanically induced fines migration. Experiments conducted on Berea cores indicated that fines migration and permeability reduction can be caused by both high fluid velocities and physicochemical effects. Therefore, it appears that there exist both a critical salt concentration and a critical flow velocity beyond which the release of fines is triggered.

In this paper the fines migration problem is analyzed following Sharma and Yortsos (1987a, b). Specifically, we consider the dynamics of the process immediately after the onset of fines migration. In a related study (Sharma et al., 1985) the corresponding regimes for the onset of clay release were experimentally delineated. The clay release region was found to occur at ionic strengths below 0.05 M, in good agreement with the critical salinity values of 0.035 M reported for Berea sandstones by Khilar and Fogler (1983) and those reported by Mungan (1965). With conditions favoring their release, the fines will migrate with the fluid and block pore throats to cause a reduction in permeability. The dynamics of this process is described by the population balance equations developed previously (Sharma and Yortsos, 1987a). In this paper we consider the solution of these population balances for the particular cases of both fines migration and fines injection.

Mathematical Formulation

We consider the process in which fine particles of size comparable to the pore size [$A = 0(1)$ in the notation of Sharma and Yortsos, 1987a] are entrained with the injected carrier fluid. The case when the particles have size much smaller than the pore size, $A \gg 1$, is of little practical interest in the absence of deposition, since it does not result in a significant permeability reduction. When $A = 0(1)$, the dominant mechanism for particle trapping is size exclusion at pore throats. In the absence of deposition ($\theta = 0$) the population balance equations (Eqs. 26–29, Sharma and Yortsos, 1987a) are reformulated for single-size particles. Introducing a new coordinate system by defining $t' = t\text{-}x$, and integrating over all particle sizes, the dimensionless governing equations become

$$\frac{\partial \rho_A}{\partial t'} = -ER\rho_A \tag{1}$$

$$\frac{\partial \rho_s}{\partial x} = ER\rho_A - \frac{1}{\mu}\frac{I(1/A)}{I(\infty)}\rho_s \tag{2}$$

$$\frac{\partial N_p}{\partial t'} = -\frac{B}{\mu}\rho_s\frac{I(1/A)}{I(\infty)} \tag{3}$$

while the population balance for pores becomes

$$\frac{\partial N_p F_p}{\partial t'} = \begin{cases} -\dfrac{B}{\mu}\rho_s\dfrac{I(r_p)}{I(\infty)}, & r_pA < 1.0 \quad (4a) \\ -\dfrac{B}{\mu}\rho_s\dfrac{I(1/A)}{I(\infty)}, & r_pA > 1.0 \quad (4b) \end{cases}$$

We note that the dimensionless parameter μ is typically very small, $\mu \ll 1$.

Comparing Eqs. 3 and 4 we also obtain

$$\frac{\partial N_p}{\partial t'} = \frac{\partial N_p F_p}{\partial t'}, \quad r_pA > 1.0 \tag{5}$$

which can be integrated further to obtain the pore size distribution for $r_pA > 1$. We get

$$F_p(r_p) = \frac{N_p - 1 + F_{po}(r_p)}{N_p}, \quad r_pA > 1.0 \tag{6}$$

hence,

$$F(1/A) = \frac{N_p - a}{N_p} \tag{7}$$

where we have defined $a = 1 - F_{po}(1/A)$, subscript o denoting initial conditions.

Equations 1–4 constitute a system of nonlinear, coupled partial differential equations, an exact solution to which is generally difficult to obtain. We elect to consider certain cases that permit simple solutions to be obtained. As indicated above, such solutions provide a useful insight into the general qualitative behavior of the process, without significant compromises in accuracy. General results and the method of solution is provided in the Appendix and in supplementary material. As a preliminary illustrative example we shall consider the solution in the case of constant R and in the absence of areal effects, that is, when the approximation $I(r) = F(r)$ is made. The underlying assumptions and implications of this approximation are discussed in later sections.

Fines Migration

Case 1. Constant R solution

When R is constant, Eq. 1 can be directly integrated. We obtain

$$\rho_A = \exp(-ERt') \tag{8}$$

Under the assumption of equal flow partition (negligible areal effects) Eqs. 2–5 become

$$\frac{\partial \rho_s}{\partial x} = ER\exp(-ERt') - \frac{1}{\mu}\rho_s F_p(1/A) \tag{9}$$

$$\frac{\partial N_p}{\partial t'} = -\frac{B}{\mu}\rho_s F_p(1/A) \tag{10}$$

$$\frac{\partial N_p F_p}{\partial t'} = \begin{cases} -\dfrac{B}{\mu}\rho_s F_p(r_p), & r_pA < 1 \\ -\dfrac{B}{\mu}\rho_s F_p(1/A), & r_pA > 1.0 \end{cases} \tag{11}$$

This system of equations yields the solution (details are provided in the supplementary material)

$$\left(\frac{N_p - a}{1 - a}\right)^a \left|\frac{N_p - 1 + w}{w}\right|^{w-1} = \exp\left[-\frac{x}{\mu}(a + w - 1)\right] \tag{12}$$

where, $w(t') = B[1 - \exp(-ERt')]$. Equation 12 provides the dependence of N_p on time and distance. Additionally, we note that the pore size distribution follows from the solution of Eq. 11 by taking the ratio of Eq. 11 and Eq. 10 and making use of the relation in Eq. 7

$$\frac{\partial N_p f_p}{\partial N_p} = \frac{f_p N_p}{N_p - a} \tag{13}$$

Equation 13 can be integrated directly to yield the pore size distribution in terms of N_p,

$$f_p(r_p, t) = \begin{cases} \dfrac{f_{po}(r_p)}{N_p}, & r_pA > 1 \\ f_{po}(r_p)\dfrac{(N_p - a)}{N_p(1 - a)}, & r_pA < 1 \end{cases} \tag{14}$$

Equation 14 serves, among other purposes, for the determination of the permeability evolution.

We next proceed with the solution of Eq. 12. Since $\mu \ll 1.0$, the sign of $(a + w - 1)$ in Eq. 12 determines the value of N_p for all values of x outside a negligibly small boundary layer of thickness μ. We distinguish two possible cases:

Case a: $B < 1 - a$. In this case, the quantity $a + w - 1$ in the exponent on the righthand side of Eq. 12 is always negative for

$t' > 0$. Accordingly, the righthand side of Eq. 12 is exponentially large. As $w - 1 < 0$ for all t', the solution of Eq. 12 is

$$N_p = 1 - w = 1 - B[1 - \exp(-ERt'] \qquad (15)$$

Equation 15 is valid for all values of x except for a boundary layer near the inlet of thickness μ. In this boundary layer, N_p rapidly varies from 1 to the value $1 - B[1 - \exp(-ERt)]$. For all practical purposes, this variation can be neglected. The resulting profiles for this case are shown schematically in Figure 1a. As time increases, the open pore density profiles decrease, the larger decrease occuring closer to the inlet of the bed. The rate of decrease is controlled by the coefficient ER, larger values of which imply larger rates of decrease. We note that in this case the open pore density never becomes smaller in value than the limiting value $1 - B > 0$, the implication being that there is not a sufficient amount of particles released to block all available pores of size smaller than $1/A$. In terms of the characteristic concentrations, the constraint for the applicability of this case reads $\rho_A^* < N_p^*(1 - a)$, in agreement with what one intuitively anticipates.

An examination of Eq. 15 also reveals that in the case of rapid fines release (i.e., $ER \gg 1$), the N_p profiles rapidly reach their limiting value $1 - B$. In such cases, we may distinguish two zones in the formation: a damaged zone in which $N_p = 1 - B$ for all $x < t$, and the original zone in which $N_p = 1$ for $x > t$. A boundary layer of order $1/ER$ separates the two zones. In any of the above cases the pore size distribution is obtained from Eq. 14 by substituting Eq. 15, while the corresponding ρ_s profiles are calculated exactly from Eq. 10. We note, however, that Eq. 10 directly implies that ρ_s is negligibly small, of order μ. We infer that the released particles are captured immediately after their release, their flowing concentration being vanishingly small.

Case b: $B > 1 - a$. In this case, the quantity $a + w - 1$ may change sign in the region of interest. A critical time t_c' exists when the above quantity becomes equal to zero. We get

$$t_c' = -\frac{1}{ER}\ln\left(1 - \frac{1-a}{B}\right) \qquad (16)$$

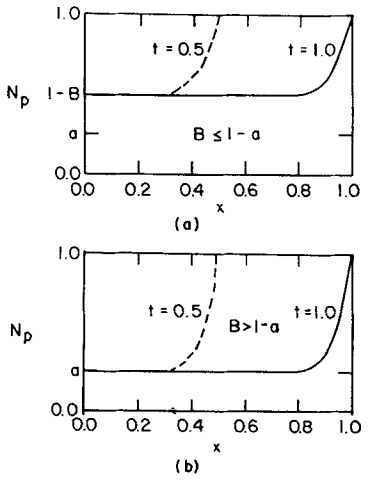

Figure 1. Open pore density profiles.
(a) $B \leq 1 - a$
(b) $B > 1 - a$.

We observe that $a + w - 1 < 0$ for $t' < t_c'$, and that $a + w - 1 > 0$ for $t > t_c'$. Therefore, the respective solutions become,

$$N_p = \begin{cases} 1 - B[1 - \exp(-ER(t - x))], & t - x < t_c' \\ a, & t - x > t_c' \end{cases} \qquad (17)$$

We observe that three zones are distinguished in the formation. The original undamaged zone ($x > t$), a moderately damaged zone of increasing length ($t - t_c' < x < t$), and a damaged zone of increasing length ($0 < x < t - t_c'$). The intermediate zone may become of negligible length in the case of large values of the parameter ER, as previously discussed. Similarly, a boundary layer of thickness μ develops for N_p at the inlet. Typical open pore density profiles obtained in this case are shown in Figure 1b. The corresponding pore size distribution is calculated directly using Eq. 14. We note that as intuitively anticipated, all pores of size $r_p < 1/A$ are blocked ($f_p = 0$) in the region where $N_p = a$. A schematic description of the evolution of the pore size distribution with time is shown in Figure 2.

Based on Eqs. 9 and 17, the suspended particle concentration ρ_s can be calculated directly. As in the previous case, the profiles are $0(\mu)$ in the intermediate zone. In the damaged zone, however, the concentration is no longer vanishingly small. To calculate the concentration profiles in this region we substitute Eq. 14 into Eq. 10 and evaluate the time derivative of N_p by making use of Eq. 12. Equation 10 is finally solved directly in terms of ρ_s. After some algebraic manipulations we obtain the solution

$$\rho_s = xER \exp[-ER(t - x)], \quad 0 < x < t - t_c' \qquad (18)$$

which is correct to order μ. Clearly, a boundary layer exists near $t - t_c'$ as the concentration drops from a finite to a vanishingly small value at the critical point. Equation 18 implies that all particles released in the damaged zone flow freely along with the injected fluid. Typical ρ_s profiles and the value of ρ_s at the effluent end ($x = 1$), where such profiles are usually monitored, are shown in Figures 3 and 4. It is to be noticed that suspended particles keep accumulating near the front $x = t - t_c'$. The concentration of particles continuously rises, and they break through the effluent end at time t^* equal to

$$t^* = 1 + t_c' \qquad (19)$$

Clearly, higher values of the release coefficient ER result in earlier breakthough times.

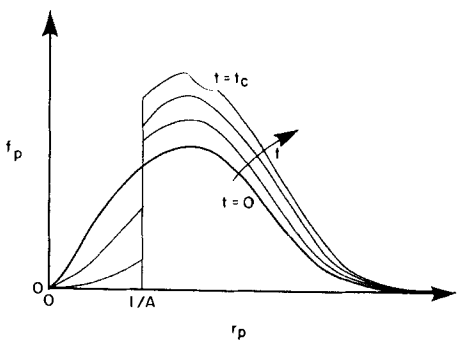

Figure 2. Pore size distribution as a function of time.

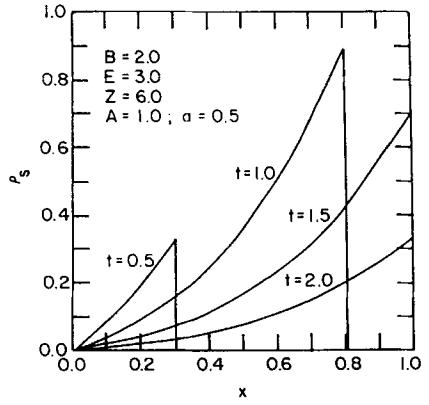

Figure 3. Suspended particle concentration profiles as a function of time.

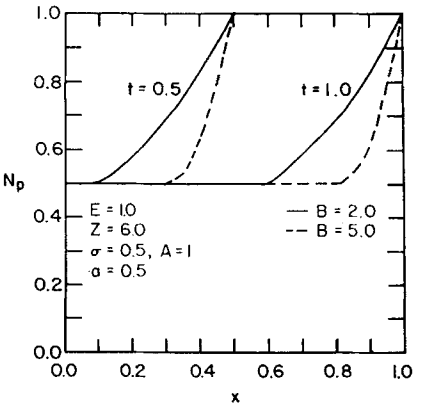

Figure 5. Open pore density profiles.

Case 2. Variable rate of release

A detailed solution to the problem can be obtained for variable R as shown in Sharma (1985) and briefly discussed in the Appendix. A computationally simpler solution follows if one assumes that pores of any size encounter the same fraction of particles. This simplification amounts to postulating $I(r_p) = F(r_p)$, that is, $u_R \propto 1/r_p^2$. The assumption appears to be reasonable for the larger pores, although it is questionable for smaller pores. Under this approximation we obtain within a constant that can be absorbed into E

$$R = N_p \tag{20}$$

The solution is,

$$N_p = \frac{(B-1)\exp[-(B-1)Et']}{B - \exp[-(B-1)Et']}, \quad N > a \tag{21}$$

The pore size distribution remains identical to Eq. 14.

The above results are graphically illustrated for a porous medium with a Gaussian initial pore size distribution of the form

$$f_{po} = \frac{\sqrt{2}}{\sqrt{\pi}\sigma} \frac{1}{\left[1 + \text{erf}\left(\frac{1}{\sigma\sqrt{2}}\right)\right]} \exp\left[-\frac{1}{2}\left(\frac{r_p - 1}{\sigma}\right)^2\right] \tag{22}$$

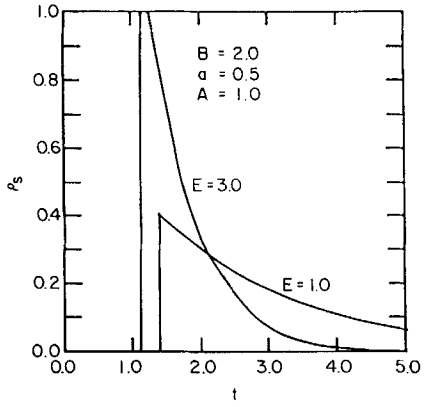

Figure 4. Effluent concentration profiles.

where σ is a dimensionless standard deviation normalized with respect to the original average pore size r_p^*. Typical pore density profiles for $A = 1$, $(a = 0.5)$, are shown in Figure 5 for different values of time and B. Based on the above, permeability can be calculated from the effective-medium theory (EMT) discussed earlier (Sharma and Yortsos, 1987a).

$$G(g) = N_p f_g(g) + (1 - N_p)\delta[g(r_p)] \tag{23}$$

and

$$f_g dg = f_p dr_p \tag{24}$$

We proceed for the estimation of g_m by substituting the expressions for N_p and f_p, Eqs. 21 and 14. After rearrangement we obtain

$$\left(\frac{N_p - a}{1 - a}\right)\int_0^{1/A} f_{po}\left(\frac{g_m - g}{g + \alpha g_m}\right)dr_p + \int_{1/A}^{\infty} f_{po}\left(\frac{g_m - g}{g + \alpha g_m}\right)dr_p = \frac{N_p - 1}{\alpha} \tag{25}$$

where $\alpha = (Z/2) - 1$. This equation is now solved numerically for g_m, hence the dimensionless local permeability k. To obtain

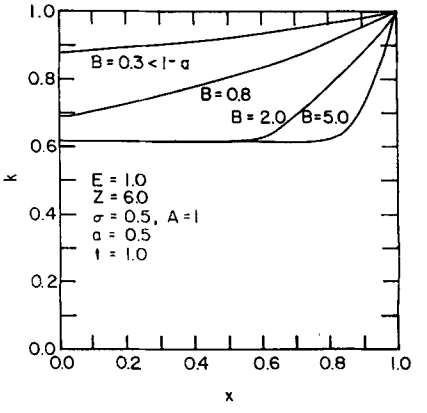

Figure 6. Local permeability profiles, effect of capture coefficient, B.

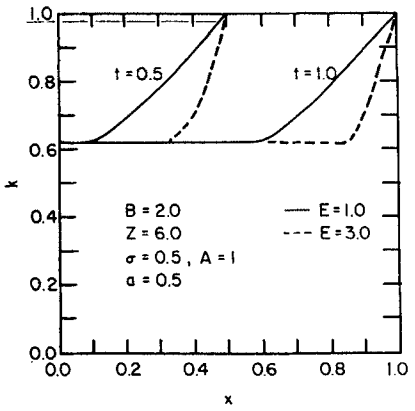

Figure 7. Local permeability profiles, effect of release, *E*.

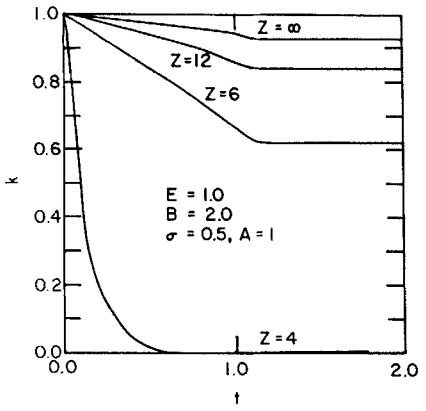

Figure 9. Overall permeability, effect of coordination number, *Z*.

the overall permeability, the harmonic mean of the local values is taken

$$\frac{1}{k(t)} = \int_0^1 \frac{dx}{k(x,t)} \tag{26}$$

Typical permeability profiles are shown in Figure 6 for a fixed value of time and various values of the parameter B. It is noticed that for low values of B such that $B < 1 - a$ ($= 0.5$ for this case), the formation damage is not very significant. Significant damage, however, occurs as the value of B increases. The effect of E is shown in Figure 7. As previously discussed, larger values of E, implying higher rates of release, result in a damaged zone of greater length. The overall medium permeability calculated from Eq. 26 is shown in Figure 8. Larger values of the parameters B and E result, in general, in lower values of permeability. It is also observed that, as anticipated, the overall permeability is less sensitive to variations in B, E than are the local values.

The effect of the coordination number on the overall permeability is shown in Figure 9. For the particular parameter values taken, the effect of the coordination number is quite significant, smaller values of Z leading to higher rates of permeability decline. It is quite evident that a network representation with a finite Z may yield significantly lower values for the permeability than a capillary tube model ($Z = \infty$). We caution, however, that this result is still subject to the assumption of negligible area effects, the region of validity of which may depend on the coordination number as well.

The generation of larger size fines causes more damage. This effect is shown in Figure 10. As indicated, an increase in the particle size, hence in the parameter A, results in a higher decline in both the local and overall values of the permeability. At this point it is also instructive to examine the final permeability of the system at large times. Plotted in Figure 11 is the final value of the overall permeability as a function of a for different values of B. When $B > 1 - a$, a single curve is followed, corresponding to $N_p = a$. However, when $B < 1 - a$, deviations from this curve occur, with smaller rates of permeability reduction for smaller values of B. We stress again the important effect of the coordination number.

Finally, we briefly consider the particular case of an initial single pore size distribution.

Case 3. Single pore size distribution

When the initial pore size distribution is unimodal

$$f_p = \delta(r_p - 1) \tag{27}$$

it remains unimodal throughout the process. In such cases the coefficient R becomes $R = N_p\beta/8$. The evolution of the pore density profiles therefore follows the same dependence as portrayed in Eq. 21, with $\beta E/8$ replacing E. We take $A < 1$, which

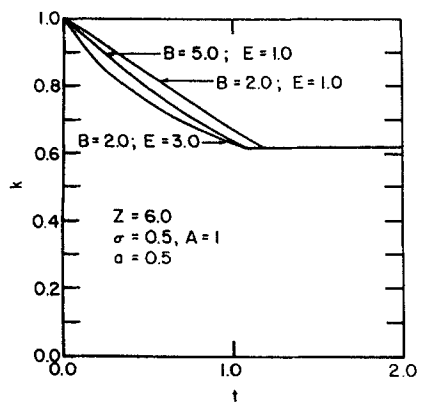

Figure 8. Overall permeability as a function of time.

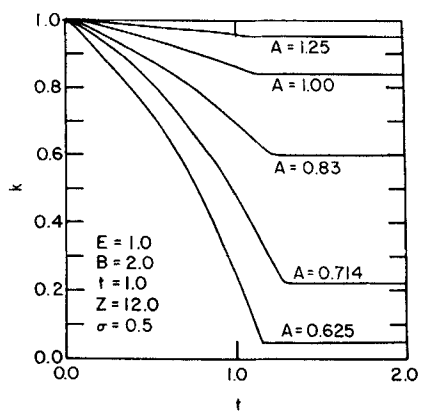

Figure 10. Overall permeability, effect of fines size.

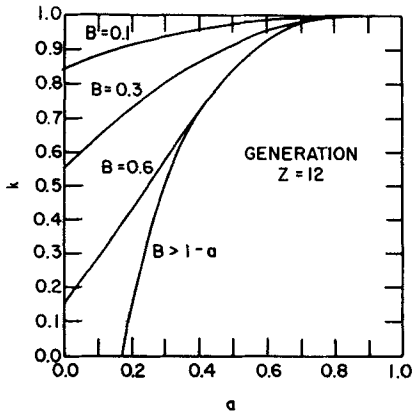

Figure 11. Final permeability value, effect of capture coefficient, B.

represents the most interesting case ($r_s^* > r_p^*$). Then $a = 0$. Accordingly, the damaged zone has all pores blocked when $B > 1$. The permeability g_m is directly calculated from Eq. 25. Noting that the distribution is given by Eq. 27, we obtain by direct substitution

$$g_m = \frac{(\alpha + 1)N_p - 1}{\alpha} \tag{28}$$

Complete plugging occurs when the percolation threshold $N_p = (\alpha + 1)^{-1}$ is reached. We readily obtain the time t^* at which g_m becomes zero

$$t^* = -\frac{8}{E\beta(B-1)} \ln \frac{B}{B(\alpha+1) - \alpha} \tag{29}$$

again indicating rapid plugging for large values of the release constant E and smaller values of the coordination number Z.

Fines Injection

To complete the presentation we also consider the problem where fine particles are injected along with the fluid, instead of being generated *in situ*. This process is different from the filtration problem discussed by Sharma and Yortsos (1987b) since here the main mechanism for particle removal is size exclusion. This situation could conceivably arise in water injection for oil recovery processes or in filtration when the injected particles are comparable in size to the pore throats.

Under the above conditions and for single-size particles, the population balance equations simplify as follows

$$\frac{\partial \rho_s}{\partial t} + \frac{\partial \rho_s}{\partial x} = -\frac{1}{\mu}\rho_s \frac{I(1/A)}{I(\infty)} \tag{30}$$

$$\frac{\partial N_p F_p}{\partial t} = \begin{cases} -\dfrac{B}{\mu}\rho_s \dfrac{I(r_p)}{I(\infty)}, & r_p A < 1 \\ -\dfrac{B}{\mu}\rho_s \dfrac{I(1/A)}{I(\infty)}, & r_p A > 1 \end{cases} \tag{31}$$

$$\frac{\partial N_p}{\partial t} = -\frac{B}{\mu}\rho_s \frac{I(1/A)}{I(\infty)} \tag{32}$$

We first consider the existence of quasi-steady state solutions in the moving coordinate

$$\xi = x - vt \tag{33}$$

Equations 30 and 31 then become

$$(1 - v)\frac{\partial \rho_s}{\partial \xi} = -\frac{B}{\mu}\rho_s \frac{I(1/A)}{I(\infty)} \tag{34}$$

$$-v\frac{\partial N_p}{\partial \xi} = -\frac{B}{\mu}\frac{I(1/A)}{I(\infty)} \tag{35}$$

which can further combine to yield

$$(1 - v)\frac{\partial \rho_s}{\partial \xi} = -\frac{v}{B}\frac{\partial N_p}{\partial \xi} \tag{36}$$

We note from Eqs. 31 and 32 that for $B = 0(1)$, the pore density at the injection point rapidly takes its limiting value $N_p = a$, since $\mu \ll 1$. Therefore, the relevant boundary conditions for Eq. 36 are

$$\rho_s = 1, \quad N_p = a, \quad \xi \to -\infty \tag{37a}$$

$$\rho_s = 0, \quad N_p = 1, \quad \xi \to +\infty \tag{37b}$$

Subsequent integration of Eq. 36 subject to the conditions of Eq. 37 yields

$$v = \frac{B}{B + 1 - a} \tag{38}$$

$$\rho_s = \frac{v(1 - N_p)}{B(1 - v)} \tag{39}$$

Equation 38 indicates that quasi-steady state solutions do exist moving with a constant velocity $0 < v < 1$. The formation now consists of two zones, a damaged zone ($0 < x < vt$) with flat profiles $\rho_s = 1$, $N_p = a$, and the original zone ($vt < x < t$) with flat profiles $\rho_s = 0$, $N_p = 1$. A boundary layer of thickness μ connects the two zones. Typical pore density profiles depicting the effect of B are shown in Figure 12. We note that the structure of the solution for the injection problem is quite similar to the generation (fines migration) problem, although much simpler to construct, since the intermediate zone is negligibly small in the present case. The permeability front that separates the two regions moves at velocity v. This simplifies the calculation of the overall permeability considerably, as the EMT calculation has to be carried out only twice. The overall dimensionless permeability is expressed as

$$k(t) = \frac{1}{\left(\dfrac{1}{k_1} - 1\right)t + 1} \tag{40}$$

where k_1 denotes as the permeability behind the front. Larger values of B cause a faster drop in permeability, Figure 13. The important effect of the coordination number is shown in Figure

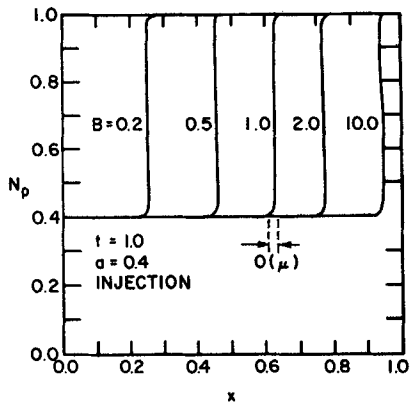

Figure 12. Open pore density profiles, effect of capture, *B*.

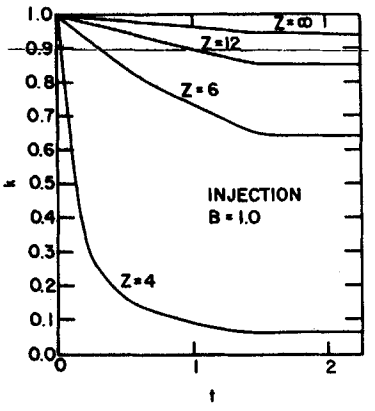

Figure 14. Overall permeability, effect of coordination number, *Z*.

14. As also anticipated, injection of larger particles causes higher formation damage, Figure 15. All numerical results are presented for a Gaussian initial pore size distribution.

We finally point out that if area effects are neglected (all pores exposed to the same fraction of particles) a closed-form solution can be obtained. A brief discussion of this case is presented below.

Negligible area effects

In this case we make use of the relationship $I(r_p) = F_p(r_p)$. The relevant population balances, with $R = 0$, become,

$$\frac{\partial \rho_s}{\partial x} = -\frac{1}{\mu}\rho_s F_p(1/A) \tag{41}$$

$$\frac{\partial N_p}{\partial t} = -\frac{B}{\mu}\rho_s F_p(1/A) \tag{42}$$

where

$$F(1/A) = \frac{N_p - a}{N_p} \tag{43}$$

These equations can now be integrated to yield the solution (Sharma, 1985),

$$\left|\frac{N_p - a}{N_{po}(t') - a}\right|^a = \left[\frac{1 - N_p}{1 - N_{po}(t')}\right]\exp\left[\frac{(1-a)}{\mu}x\right] \tag{44}$$

where N_{po} satisfies

$$N_{po} + a\ln(N_{po} - a) = -\frac{B}{\mu}t' + 1 + a\ln(1 - a) \tag{45}$$

The solution in Eqs. 44 and 45 can be used to verify the existence of the quasi steady states, as well the boundary layer behavior near the front $x = vt$. For simplicity, such details are not presented here.

Conclusions

When the mechanism for particle trapping is size exclusion, formation damage due to fines migration is a sensitive function of the release, *R*, and capture, *B*, coefficients, which involve the flow rate and the amount of particles available for release, and the pore size distribution of the porous medium. For relatively large values of *B*, the formation consists of three zones: a damaged zone, an intermediate moderately damaged zone, and the original formation. As the release coefficient is increased, the

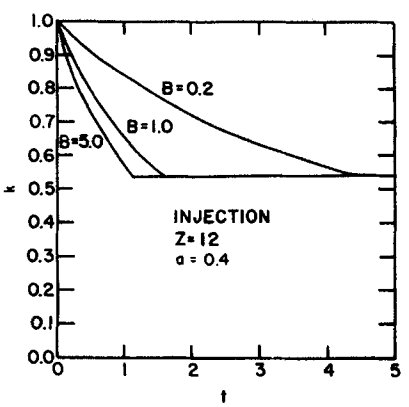

Figure 13. Overall permeability, effect of capture coefficient, *B*.

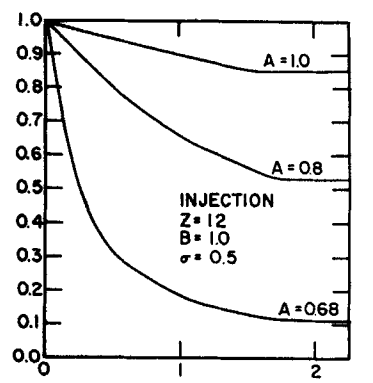

Figure 15. Overall permeability, effect of particle size.

intermediate zone becomes smaller in length. The location of these zones is explicitly calculated as a function of time and the process parameters. The permeability reduction is quantitatively expressed using a network model and the effective-medium theory. It is found that the permeability is a sensitive function of the coordination number of the network and the particle size. Computationally simple results are obtained for several simple processes under the assumption of single-size particles. A general method is also developed for the solution of more general processes.

The related problem of filtration of relatively large particles is analyzed. It is found that when the mechanism for retention is size exclusion, an internal filter cake of increasing length develops within the filter bed. The rate of growth of the filter cake is evaluated for the case of single-size particles. Expressions for the evolution in time of the permeability of the filter bed are developed in terms of the particle and pore sizes.

The results obtained find application in the prediction and prevention of formation damage in fines migration in oil recovery processes, and in the filtration of large particulates. The analysis may also be extended to related processes of size exlcusion chromatography and emulsion flow in porous media.

Notation

a = fraction in open pores
A = parameter, r_p^*/r_t^*
B = capture coefficient, defined in Sharma and Yortsos (1987a)
E = release coefficient, defined in Sharma and Yortsos (1987a)
f = size distribution
F = integral of size distribution
g = pore conductance
G = conductance distribution
k = permeability
N = open pore density
r_p^* = pore size
r_t^* = particle size
R = release coefficient
t = time
t' = transformed time
u_R = velocity in pore of size r_p
v = velocity
x = distance
Z = coordination number

Greek letters

α = parameter, $Z/2 - 1$
β = parameter, g_{mo}
μ = paramter, ratio of pore to medium length, defined in Sharma and Yortsos (1987a)
ξ = moving coordinate
ρ = concentration

Subscripts

A = attached
c = critical
F = final
m = effective
o = initial
p = pore
s = suspended

Superscript

$*$ = dimensional

Appendix: Variable R—General Results

In seeking a solution to the general problem we are guided by the preceding analysis and take advantage of the existence of the small parameter μ. An order-of-magnitude analysis of Eq. 2 reveals that either ρ_s or $I(1/A)$ is of order μ. As also suggested by the above discussion, we anticipate that in some regions of the x, t space any one of the two conditions will always prevail.

In the regions where $\rho_s = 0(\mu)$, we define $\rho_{sm} = \rho_s/\mu$ and rewrite Eq. 2 in the form

$$\frac{\partial \rho_{sm}}{\partial x} = ER\rho_A - \rho_{sm}\frac{I(1/A)}{I(\infty)} \tag{A1}$$

Assuming that $I(1/A)$ is 0(1), which in view of Eq. 7 implies $N_p > a$, the solution of Eq. A1 outside some negligible boundary layers is

$$\frac{\rho_s}{\mu}\frac{I(1/A)}{I(\infty)} = ER\rho_A \tag{A2}$$

Further substitution of Eq. A2 into Eq. 3 leads to

$$\frac{\partial N_p}{\partial t'} = -BER\rho_A = B\frac{\partial \rho_A}{\partial t'} \tag{A3}$$

where for the second equality use is made of Eq. 1. Equation A3 can be integrated in time. We obtain

$$\rho_A = 1 + \frac{N_p - 1}{B} \tag{A4}$$

which provides an algebraic relationship between ρ_A and N_p. Further substitution of Eq. A4 into Eq. A3 and the results of Eq. 4a into the two equations in terms of N_p and F_p results in:

$$\frac{\partial N_p}{\partial t'} = -ER(B - 1 + N_P) \tag{A5}$$

$$\frac{\partial N_p}{\partial t'} = -ER(B - 1 + N_P)\frac{I(r_p)}{I(1/A)}, \quad r_pA < 1.0 \tag{A6}$$

We remark that for $r_pA > 1.0$ the pore size density is still given by Eq. 6. We also note that by definition R is a unique function of N_p and f_p (thus F_p). The system of Eqs. A5, A6, and 6 can in principle be solved to provide the desired dependence of N_p and F_p on time and distance. In particular, it is evident from Eqs. A5 and A6 that the dependence of F_p on time enters implicitly through the variable N_p. In the supplementary material we outline a method for calculating F_p, which for the general case may involve a considerable amount of computation.

Having determined F_p, the coefficient R is expressed as a function of N_p. R is positive and explicitly proportional to N_p (although an additional dependence also enters through the integral term.) Nevertheless, some general results can be obtained.

We proceed by integrating Eq. A5 in the form

$$\int_1^{N_p} \frac{dN_p}{R(N_p)(B + N_p - 1)} = -Et' \tag{A7}$$

Two cases are distinguished. When $B < 1 - a$, the integral diverges at the value $N_p = 1 - B$. Therefore, N_p decreases as t' increases, approaching asymptotically in t' the limiting value $1 - B$. The formation consists of two zones, the original un-

damaged zone ($x > t$), and a moderately damaged zone ($x < t$), in identical qualitative agreement with the case of constant R discussed previously. The previous discussion remains identical for the present case as well, with the understanding that the shape of the profiles would be slightly modified when the actual function $R(N_p)$ is used in Eq. A7. On the other hand, when $B > 1 - a$, the denominator in Eq. A7 is always positive, indicating that as t' increases, N_p continuously decreases. At the critical point t'_c, N_p reaches the limiting value a. This point marks the end of the validity of Eq. A7, since $F_p(1/A)$ becomes equal to zero and ρ_s is not negligibly small any longer. The critical value t'_c is calculated from Eq. A7

$$t'_c = t - x_c = \frac{1}{E}\int_a^1 \frac{dN_p}{R(N_p)(B + N_p - 1)} \qquad \text{(A8)}$$

from which the location of the boundary x_c, where the open pore density has reached its minimum value a, can be calculated. As in the previous case of constant R, this limiting boundary travels with the fluid velocity, lagging behind by a constant value. When the particle release is fast ($E \gg 1$), the intermediate, moderately damaged zone is of very small length. Again, the entire discussion of the constant R case is very much pertinent to the present general case.

We finally note that in the damaged zone ($0 < x < t - t'_c$) the released particle concentration can also be calculated. To this effect, we combine Eqs. 2 and 3

$$\frac{\partial \rho_s}{\partial t'} = ER\rho_A + \frac{1}{B}\cdot\frac{\partial N_p}{\partial t'} \qquad \text{(A9)}$$

and note that in the damaged zone both N_p and f_p are constant. Accordingly, R is also constant, $R = R_F$, subscript F denoting final values. With constant R, Eq. 1 can be integrated to yield

$$\rho_A = \rho_{Ac} \exp\left[-ER_F(t' - t'_c)\right] \qquad \text{(A10)}$$

where ρ_{Ac} is the concentration at the critical point calculated from Eq. A5 by setting $N_p = a$. We obtain

$$\rho_A = \frac{(B - 1 + a)}{B} \exp\left[-ER_F(t' - t'_c)\right] \qquad \text{(A11)}$$

Expression A11 can now be substituted into Eq. A9. Recalling that N_p is constant, we get

$$\frac{\partial \rho_s}{\partial x} = ER_F \frac{(B - 1 + a)}{B} \exp\left[-ER_F(t' - t'_c)\right] \qquad \text{(A12)}$$

which can be integrated to yield

$$\rho_s = xER_F \frac{(B - 1 + a)}{B} \exp\left[-ER_F(t' - t'_c)\right] \qquad \text{(A13)}$$

As expected, Eq. A13 reduces to Eq. 18 when R remains constant throughout the process. We again observe the accumulation of particles near the front x_c, where a sharp boundary-layer type discontinuity develops for ρ_s. Suspended particles break through the production end at the dimensionless time $1 + t'_c$. The effluent profiles have a qualitatively similar shape to those in Figure 4.

Literature Cited

Gabriel, G. A., and G. R. Inamdar, "An Experimental Investigation of Fines Migration in Porous Media," Paper No. 12168, 58th SPE Ann. Meet., San Francisco (Oct., 1983).

Gray, D. H., and R. Rex, "Formation Damage in Sandstones Caused by Clay Dispersion and Migration," *Proc. 14th Nat. Conf. Clays and Clay Minerals*, 355 (1966).

Gruesbeck, C., and R. E. Collins, "Entrainment and Deposition of Fine Particles in Porous Media," *SPE J.*, 847 (1982).

Jones, F. O., "Influence of Chemical Composition of Water on Clay Blocking of Permeability," *Trans. AIME*, **231**, 441 (1964).

Khilar, K. C., "The Water Sensitivity of Sandstones," Ph.D. Thesis, Univ. Michigan, Ann Arbor (1981).

Khilar, K. C., and H. S. Fogler, "Water Sensitivity of Sandstones," *SPE J.*, 55 (1983).

———, "The Existence of a Critical Salt Concentration for Particle Release," *J. Colloid Interf. Sci.*, **101**, 214 (1984).

Khilar, K. C., H. S. Fogler, and J. S. Ahlawalia, "Sandstone Water Sensitivity: Existence of a Critical Rate of Salinity Decrease," *Chem. Eng. Sci.*, **38**, 789 (1983).

Moore, J. E., "Clay Mineralogy Problems in Oil Recovery," *Pet. Eng.*, **32**, 78 (1960).

Mungan, N., "Permeability Reduction Through Changes in pH and Salinity," *J. Pet. Tech.*, 1449 (1965).

———, "Permeability Reduction Due to Salinity Changes," *J. Canad. Pet. Tech.*, **20**, 113 (1968).

Sharma, M. M., "Transport of Particulate Suspensions in Porous Media: Application to Filtration and Fines Migration in Sandstones," Ph.D. Diss. Univ. So. California (1985).

Sharma, M. M., and Y. C. Yortsos, "Transport of Particulate Suspensions in Porous Media: Model Formulation," *AIChE J.*, 33(10), 1636 (Oct., 1987a).

———, "A Network Model for Deep Bed Filtration Processes," *AIChE J.*, 33(10), 1644 (Oct., 1987b).

Sharma, M. M., Y. C. Yortsos, and L. L. Handy, "Deposition and Release of Clays in Sandstones," SPE Paper 13572, SPE Symp. Oilfield and Geothermal Chem., Phoenix (1985).

Manuscript received June 10, 1985, and revision received May 27, 1987.

See NAPS document No. 04526 for 13 pages of supplementary material. Order from NAPS c/o Microfiche Publications, P.O. Box 3513, Grand Central Station, New York, NY 10163. Remit in advance in U.S. funds only $7.75 for photocopies or $4.00 for microfiche. Outside the U.S. and Canada, add postage of $4.50 for the first 20 pages and $1.00 for each of 10 pages of material thereafter, $1.50 for microfiche postage.